ChemComm

Accepted Manuscript

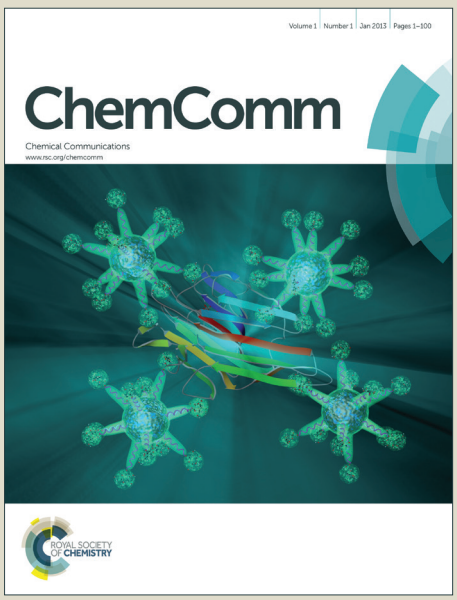

ROYAL SOCIETY OF CHEMISTRY

www.rsc.org/chemcomm

Generation of spatiotemporal calcium patterns through coupling a pH-oscillator to a complexation equilibrium†

István Molnár,[a] Krisztina Kurin-Csörgei,[a] Miklós Orbán,[a] and István Szalai*[a]

Received Xth XXXXXXXXXX 20XX, Accepted Xth XXXXXXXXX 20XX
First published on the web Xth XXXXXXXXXX 200X
DOI: 10.1039/b000000x

Sustained spatiotemporal pH and calcium patterns are produced in a non-equilibrium inorganic reaction-diffusion system by coupling two modules, the bromate-sulfite-ferrocyanide pH-oscillator and the pH-sensitive complexation of Ca^{2+} by ethylenediaminetetraacetate. The development of chemical waves is mainly determined by the oscillatory module, however the formation of the localised stationary like patterns results in the synergistic interaction between the modules.

Traditionally, chemistry deals with the description of our material word by means of analytical or physico-chemical methods and with the synthesis of new compounds. However, chemistry is capable of building functioning systems, which are set in action by sustained reaction networks, and show complexity and emergent phenomena. Systems chemistry[1] covers the different approaches, which have developed for studying such chemical complexity.

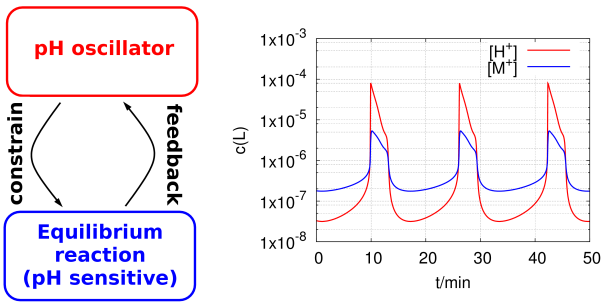

Fig. 1 Design scheme of the coupled oscillatory system (a), and simulated concentration *vs.* time curves of the autocatalytic (H^+) and the target species (M^+) in an OSFR (b). Here $c(L)$ is the concentration at the furthermost point from the feeding surface. For the details of the reactor configuration and the simulations see ESI.†

[a] *Institute of Chemistry, Eötvös Loránd University, Budapest, Hungary. Fax: +36-1-372-25-92; Tel: +36-1-3722500/1902 ; E-mail: szalai.istvan@chem.elte.hu*

† Electronic Supplementary Information (ESI) available: Experimental and simulation methods & movies of spatiotemporal oscillations. See DOI: 10.1039/b000000x/

Here, we present a dynamical system operated by an oscillatory reaction that is linked to a complexation equilibrium and produces spatiotemporal patterns of a target species which is not included in the core oscillatory process. In this arrangement the complexation equilibrium follows the constraint of the oscillatory reaction, but it also provides a feedback on its operation (Fig. 1a). pH-oscillators[2] are preferably used to develop such type of coupled systems, where a pH-sensitive equilibrium follows the periodic changes in the hydrogen ion concentration but usually the feedback of the linked equilibrium is neglected.[3,4] The skeleton mechanism of a two-substrate pH-oscillators consists of the following three steps:[5]

$$A^- + H^+ \rightleftharpoons HA \qquad \text{(R1)}$$

$$B + HA \xrightarrow{H^+} H^+ + P \qquad \text{(R2)}$$

$$C + H^+ \longrightarrow Q \qquad \text{(R3)}$$

Here B stands for the oxidant, A^- and C, denote the two substrates, P and Q are the products. This is an activator-inhibitor type system, where (R1)-(R2) represents the (+)feedback, while (R3) provides the (−)feedback. In the experiments sulfite ions are most often used as component A^-, the typical oxidant is iodate, bromate or hydrogen peroxide, and C can be ferrocyanide, thiourea, carbonate ions etc. Besides temporal oscillations, formation of pH waves and stationary patterns have also been observed in some of these reactions.[6,7] Following the idea of Orbán and coworkers,[4] we linked a pH sensitive complexation equilibrium (R4)-(R5) to the oscillatory module (R1)-(R3) to produce spatiotemporal patterns in $[M^+]$.

$$S^- + M^+ \rightleftharpoons MS \qquad \text{(R4)}$$

$$S^- + H^+ \rightleftharpoons HS \qquad \text{(R5)}$$

In the experiments ethylenediaminetetraacetate (EDTA) was used to bind Ca^{2+} as the target species. Numerical simulations using equations (R1)-(R5) demonstrate, that under appropriate conditions the spatiotemporal oscillations of $[H^+]$ are followed by the periodic changes of $[M^+]$ (Fig. 1b) in an open one side fed reactor (OSFR). The key step of the experimental

realization of this type of coupled system is the selection of the proper oscillator, that is capable of producing robust driving force, namely large enough amplitude pH-oscillations to induce significant back and forth shifts in reactions (R4)-(R5). From stoichiometric point of view the use of high concentration of A^- is preferred, since the magnitude of the pH drop (ΔpH) during the autocatalytic process (R1)-(R2) increases with the initial concentration of A^- and independent form the nature of the oxidant, according to the equation derived previously: $\Delta pH = -(pK_{HA} + \log[A^-]_0)$.‡[8] However, the development of oscillations requires a suitable balance between the rate of the $(+)$ and the $(-)$feedbacks, and the increase of $[A^-]_0$ might improperly speed up the autocatalytic process. Accordingly, robust large amplitude pH-oscillations are expected by using a sluggish oxidant and relatively high amount of A^-. The oscillators based on the bromate-sulfite (BS) autocatalytic reaction provide the best fit for the above requirements, e.g by adding ferrocyanide as a second substrate (BSF reaction). Concerning the complexation module, S^- must be protonated at the low pH phase of the oscillations and bind the target species at the high pH phase. The presence of S^- gives rise to substantial feedback on the dynamics of the oscillator due to its buffering effect and the slowing down in the overall rate of the $(+)$feedback process. Additionally, in spatially distributed systems, if the mobility of S^- is low compared to the other species, the decrease in the effective diffusion of H^+ comes also into play. It is recommended to apply an $[S^-]_0$ that is lower than $[H^+]_0$ to keep the feedback on an acceptable level.[8]

Spatiotemporal patterns in the BSF pH-oscillator have not been reported previously. In a continuous flow stirred tank reactor (CSTR) the BSF reaction shows bistability and oscillations between pH ~ 3 and ~ 6.5.[9] To generate pH patterns we used the design method, which has been successfully applied in analogous systems.[7] This method starts with finding spatial bistability. The experiments were performed in an OSFR, which consists of a thin disc-shaped piece of agarose gel, in contact with the contents of a CSTR through one face (Fig. S1, ESI†). The gel quenches any convective fluid motion and allows an undisturbed development of the reaction-diffusion patterns in its core. The reagents and products are diffusively exchanged at the contact surface with the CSTR. The spatial structure developed when the CSTR content was in the low extent of reaction steady state to insure far-from-equilibrium conditions at the feed boundary of the OSFR. In the absence of ferrocyanide formation of propagating pH fronts was observed (Fig. S2, ESI†), a phenomenon that typically develops in bistable reaction-diffusion systems. The front connects two stationary state domains, denoted as *F* (flow)- and *M* (mixed)-states of the gel. At the *F*-state the extent of reaction is low within the gel, thus the pH is high. However, at the *M*-state, in the depth of the gel, the extent of the reaction turns high and correlatively the pH is low. The existence of spatial bistability in the BS reaction has already been reported. Due to the kinetic complexity of the BS reaction at the ratios of $[BrO_3^-]_0/[SO_3^{2-}]_0 > 2$, a narrow domain of spatiotemporal oscillations was also observed.[10] However, in our experiments this ratio is below one, therefore the $(-)$feedback provided by reaction (R3) is necessary for the development of spatiotemporal patterns. As the influence of reaction (R3) reaches a critical level, e.g. $[K_4Fe(CN)_6]_0 \geq 10$ mM, spatiotemporal pH-oscillations form spontaneously (Fig. 2). The

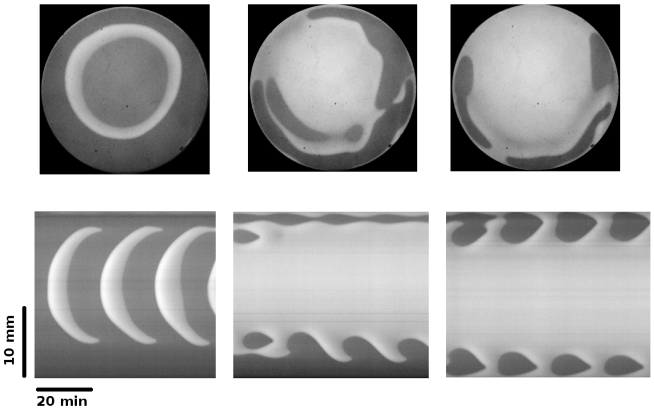

Fig. 2 pH patterns of the BSF reaction observed in an OSFR. Snapshots and the corresponding time-space plots of spatiotemporal waves at $[H_2SO_4]_0 = 7.4$ mM (a,b) and localised oscillations at $[H_2SO_4]_0 = 7.5$ mM (c,d) and at $[H_2SO_4]_0 = 7.6$ mM (e,f). To visualise the patterns bromocresol green indicator was used. On the pictures dark and light colours correspond to the F- and the *M*-states, respectively. The experimental conditions: $[NaBrO_3]_0 = 65$ mM, $[Na_2SO_3]_0 = 80$ mM, $[K_4Fe(CN)_6]_0 = 30$ mM, $T = 30$ °C and $\tau = 500$ s. For the experimental details and movies see ESI.†

state of the system and the appearance of the wave phenomena depend on the $[H_2SO_4]_0$. Only the homogeneous *F*-state is observed if $[H_2SO_4]_0 \leq 7.3$ mM. At $[H_2SO_4]_0 = 7.4$ mM the oscillation begins with the spontaneous growth of an *M*-state domain at the center of the reactor. The *M*-state domain expands in all directions, but the motion of this $(+)$front (transition from F- to *M*-state) slows down and stops at a finite distance from the rim of the disc. In the meanwhile, inside the *M*-state domain the *F*-state reappears and a sharp $(-)$front (transition from M- to *F*-state) starts to follow the $(+)$front (Fig. 2a and b). The two fronts annihilate each other when they collide. At higher $[H_2SO_4]_0$ the center part of the disc settles in the *M*-state, while oscillations develop around the stationary *M*-state domain (Fig. 2c,d,e and f). In all cases the dynamics is governed by the motion of the $(+)$ and $(-)$fronts (Fig. S3, ESI†). When $[H_2SO_4]_0 \geq 7.7$ mM, the gel content settles in

‡ Here, $[X]_0$ denotes the input feed concentration of species X.

the *M*-state. According to the work of Orbán and coworkers,[4] temporal oscillations in the $[Ca^{2+}]$ can be induced by adding CaEDTA to the BSF reaction in a CSTR. To visualise the variation in the $[Ca^{2+}]$ arseneazo III indicator was used. The Ca^{2+} complex of arseneazo III has a characteristic absorbance maximum at $\lambda = 650$ nm (Fig. S3, ESI†). Although, the indicator is pH sensitive, at this wavelength the effect of pH on the absorbance is negligible. The presence of CaEDTA causes a shift in the pH of the input flow, thus spatiotemporal patterns form at lower $[H_2SO_4]_0$, than in its absence. In the coupled system the *F*-state of the gel is characterised by low $[Ca^{2+}]$, since Ca^{2+} is bound to EDTA, but at the *M*-state in depth of the gel the $[Ca^{2+}]$ is relatively high. At $[H_2SO_4]_0 = 6.8$ mM spatiotemporal oscillations develop (Fig. 3a and b), similar to the ones shown in Fig. 2a and b. The difference is, that the

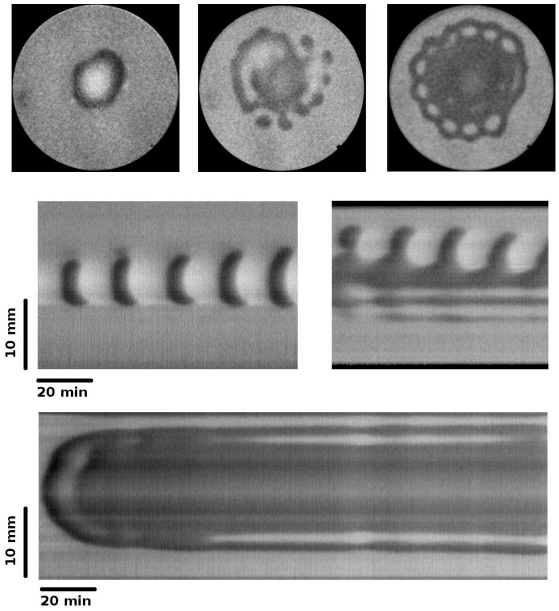

Fig. 3 Ca^{2+} patterns of the BSF-CaEDTA reaction observed in an OSFR at $[CaEDTA]_0 = 2.0$ mM. Snapshots and the corresponding time-space plots of spatiotemporal waves at $[H_2SO_4]_0 = 6.8$ mM (a,b), localised oscillations at $[H_2SO_4]_0 = 6.9$ mM (c,d) and at $[H_2SO_4]_0 = 7.0$ mM (e,f). On the pictures the light and dark colours correspond to the F- (low $[Ca^{2+}]$) and M (high $[Ca^{2+}]$) states, respectively. The other experimental conditions are the same like in Fig 2. Movie is available in ESI.†

propagation of the $(+)$front stops far from the rim of the disc, thus the wave phenomenon is more localised to the center of the reactor. At $[H_2SO_4]_0 = 6.9$ mM the center part of the disc stays in the stationary *M*-state, and oscillations appear around it (Fig. 3c and d). Additionally, a few separated high $[Ca^{2+}]$ spots remain stable close to the central *M*-state domain, as it is indicated by the horizontal lines in Fig. 3d. The further increase in $[H_2SO_4]_0$ leads to the formation of a large *M*-state domain, that is unstable and inside it a row of low $[Ca^{2+}]$ spots appear around its rim (Fig. 3e), that appear as light gray horizontal lines in Fig. 3f. The arrangement of the spots bears resemblance to the Turing patterns.[11]

In conclusion, sustained spatiotemporal patterns have been observed in the BSF reaction, especially in form of localised waves under the conditions we have explored. Localised patterns represent isolated structures of one state embedded in a domain of another state and usually appear in bistable systems,[12] but they can also be originated in the sensitivity of the system to gradients of parameters, e.g. to a small ramp in the thickness of the gel. The formation of stationary patterns is expected when the diffusion coefficient of the inhibitor exceeds that of the activator. In the coupled BSF-CaEDTA system the stabilization of localised spots indicates that the feedback of the CaEDTA equilibrium slows down the effective diffusivity of hydrogen ions, most likely due to a possible interaction of CaEDTA with the agarose matrix. Our results show the importance of interaction between the driving and the driven modules in this type of coupled systems, which might be also relevant in biology, where oscillatory process, e.g Ca^{2+} oscillations,[13] are naturally linked to complexation equilibria.

We thank the support of the Hungarian Scientific Research Fund (OTKA 100891).

References

1 R. F. Ludlow and S. Otto, *Chem. Soc. Rev.*, 2008, **37**, 101–108.
2 G. Rábai, M. Orbán and I. R. Epstein, *Acc. Chem. Res.*, 1990, **23**, 258–263.
3 (*a*) R. Yoshida, H. Ichijo, T. Hakuta and T. Yamaguchi, *Macromol. Rapid Comm.*, 1995, **16**, 305–310; (*b*) C. J. Crook, A. Smith, R. A. L. Jones and A. J. Ryan, *Phys. Chem. Chem. Phys.*, 2002, **4**, 1367–1369; (*c*) I. Varga, I. Szalai, R. Mészaros and T. Gilányi, *J. Phys. Chem. B*, 2006, **110**, 20297–20301; (*d*) T. Liedl, M. Olapinski and F. C. Simmel, *Angew. Chem. Int. Edit.*, 2006, **45**, 5007–5010; (*e*) I. Lagzi, B. Kowalczyk, D. Wang and B. A. Grzybowski, *Angew. Chem.*, 2010, **122**, 8798–8801.
4 K. Kurin-Csörgei, I. R. Epstein and M. Orbán, *Nature*, 2005, **433**, 139–142.
5 G. Rábai, *ACH Models in Chemistry*, 1998, **135**, 381–392.
6 (*a*) K. Lee, W. Mccormick, Q. Ouyang and H. Swinney, *Science*, 1993, **261**, 192–194; (*b*) I. Szalai and P. De Kepper, *Chaos*, 2008, **18**, 026105.
7 (*a*) J. Horváth, I. Szalai and P. De Kepper, *Science*, 2009, **324**, 772–775; (*b*) I. Szalai, J. Horváth, N. Takács and P. De Kepper, *Phys. Chem. Chem. Phys.*, 2011, **13**, 20228–20234; (*c*) H. Liu, J. A. Pojman, Y. Zhao, C. Pan, J. Zheng, L. Yuan, A. K. Horváth and Q. Gao, *Phys. Chem. Chem. Phys.*, 2012, **14**, 131–137.
8 I. Molnár, N. Takács, K. Kurin-Csörgei, M. Orbán and I. Szalai, *Int. J. Chem. Kinet.*, 2013, **45**, 462–468.
9 E. C. Edblom, Y. Luo, M. Orban, K. Kustin and I. R. Epstein, *J. Phys. Chem.*, 1989, **93**, 2722–2727.
10 Z. Virányi, I. Szalai, J. Boissonade and P. De Kepper, *J. Phys. Chem. A*, 2007, **111**, 8090–8094.
11 A. Turing, *Phil. Trans. R. Soc. B*, 1952, **237**, 37–72.
12 V. K. Vanag and I. R. Epstein, *Chaos*, 2007, **17**, 037110.
13 L. Leybaert and M. J. Sanderson, *Physiol. Rev.*, 2012, **92**, 1359–1392.